

*THEORETICAL AND EXPERIMENTAL INVESTIGATION OF RADIATION PULSATON
FROM A CO₂ LASER WITH A NONLINEAR ABSORBING CELL*

Yu. V. BRZHAZOVSKIĬ, L. S. VASILENKO, S. G. RAUTIAN, G. S. POPOVA and V. P. CHEBOTAEV

Institute of Semiconductor Physics, Siberian Division, USSR Academy of Sciences

Submitted August 21, 1970

Zh. Eksp. Teor. Fiz. 61, 500—510 (August, 1971)

Results are presented of an experimental and theoretical investigation of the conditions for the appearance of regular radiation pulsations from a CO₂-He-N₂ laser with an internal absorbing cell filled with CO₂ at a temperature of 800° K. A typical radiation pulse duration was ~ 10 μsec and its intensity exceeded the continuous generation level by approximately an order of magnitude. The pulse repetition frequency varied from several tens of Hz to 50–60 kHz, depending on the excitation level of the discharge tube. The stability of the stationary conditions of the resonator field is investigated theoretically by taking into account the effect of the collisions on the molecule-velocity distribution and the rotational-quantum-number distribution (in the strong-collision model). Numerical calculations of the upper boundary for an unstable regime are qualitatively in agreement with the experimental data.

1. INTRODUCTION

It is known that in solid-state lasers the introduction of a nonlinear absorber (a saturable filter) into the resonator leads to the occurrence of a giant-pulse regime. This interesting phenomenon has been the subject of a large number of investigations^[1]. In gas lasers, the regime of regular pulsations was first obtained by introducing into the resonator of a CO₂ laser an absorbing cell with SF₆^[2]. Soon afterwards, a similar regime was observed by introducing BCl₃^[3] and CO₂^[4,5] as absorbers. By now there is a sufficiently wide assortment of gases, the introduction of which in an absorbing cell leads to pulsed lasing (see, for example, ^[6-8]).

Even in the earlier investigations^[9-11] of gas lasers with nonlinear absorbers, attention was called to a phenomenon of a different type, namely, instability of the hysteresis type. Finally, under certain conditions the nonlinear absorption leads to the occurrence of angular power pulsations.

The giant-pulse regime in a solid-state laser with saturable filter, hysteresis phenomena, and the regime of regular pulsations in a gas laser with nonlinear absorber have some features in common, since these phenomena are based on a decrease of the absorption in a strong field. Nonetheless, investigations performed with an absorbing cell with CO₂ have revealed the presence of unique phenomena inherent only to gas lasers. An investigation of the influence of collisions on the character of the saturation of the laser transitions in CO₂^[5] has shown that the homogeneous character of the saturation at relatively low pressures (0.5–1 Torr), typical of the absorbing cell, is due to collisions that change the velocity of the molecule and the rotational quantum number. It was also shown that after a sudden turning on of the field, the saturation changes from inhomogeneous to homogeneous within a certain characteristic time. As will become clear from the following, this circumstance plays an important role in the explanation of the mechanism of occurrence of regular

pulsations. It should be noted that in^[5] the absorbing cell was introduced in order to obtain a narrow dip in the saturated absorption line. The occurrence of pulsation in this case was a serious obstacle to research aimed at developing a highly-stabilized CO₂ laser. Naturally, it became necessary to investigate theoretically and experimentally the regime of regular pulsations in the gas laser with absorbing cell.

Yakubovich and Bepalov^[12] investigated the stability of a laser with an absorbing cell. As the model describing the behavior of the atom, they used the simplest two-level system and assumed the atoms to be immobile. In addition, they assumed that the relaxation time of the dipole moment of the medium is much shorter than all the other times characterizing the system. It follows from the statements made above that the model assumed in^[12] does not take into account a factor of very great importance for molecular gas lasers, namely rotational relaxation.

In the present paper we have chosen as the investigated model a molecular system with a simple vibrational-rotational spectrum, corresponding, for example, to the spectrum of the CO₂ molecule. The lasing is on a transition between two vibrational-rotational levels, but unlike in^[12] account is taken of the collision exchange between the vibrational sublevels and of the Doppler broadening as a result of the thermal motion of the molecules. A theoretical analysis of this model and the experimental data have shown that the main cause of the occurrence of regular pulsations are the collisions that lead to an intense "mixing" of the velocities and rotational sublevels of the molecules.

2. EXPERIMENTAL INVESTIGATION OF THE INSTABILITY REGION

The experimental setup (see Fig. 1) consisted of a rigidly mounted laser of length $L = 120$ cm. The resonator mirrors and the diameter of the discharge tube ($d = 12$ mm) were chosen such that only axial oscillation modes were generated. The resonator could be tuned

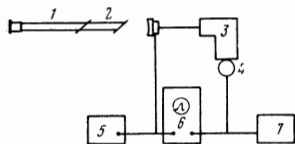


FIG. 1

FIG. 1. Diagram of experimental setup: 1—laser tube, 2—absorbing cell, 3—monochromator, 4—photoresistor, 5—acoustic generator, 6—cathode-ray oscilloscope, 7—pulse counter.

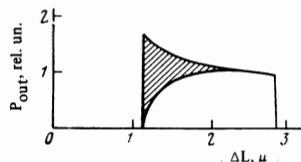


FIG. 2

FIG. 2. Dependence of the output power on the resonator length. $P(20)$ line of the $00^0 1-10^0 0$ transition of CO_2 .

over a range $c/2L$ with the aid of a piezoceramic. The active length of the discharge was 60 cm and the length of the absorbing cell about 30 cm. The active part was filled with a $\text{CO}_2\text{-N}_2\text{-He}$ mixture at a total pressure of ~ 10 Torr. The presence of strong competition between the rotational sublevels has caused the emission spectrum of our laser to consist at each instant of time of one mode on one vibrational-rotational transition. An investigation of the regime of the spontaneous pulsations was carried out on the $P(20)$ line, because generation on this line was observed in a relatively broad spectral interval (approximately ± 20 MHz relative to the line center). The resonator line was scanned at a frequency 10–12 Hz. The time resolution of the recording system was better than $1 \mu\text{sec}$. The signal from the photoresistor was fed either to the input of an oscilloscope or to a pulse counter.

Depending on the absorption (i.e., on the pressure and temperature of the absorbing cell) and on certain other conditions, two pulsation regimes were observed, damped and undamped.

Figure 2 shows the behavior of the output power as a function of the natural frequency of the resonator following introduction of 0.7–0.9% absorption (0.25 Torr of CO_2 at a cell-wall temperature 800°K). At the instant when lasing starts on the given transition, characteristic damped power oscillations appear, with frequency 40–50 kHz; the region in which the damped oscillations were observed is shown shaded in Fig. 2. An increase of the absorption (to 1.2–2.5%) causes the region where the oscillations are observed to extend closer to the line center, and at sufficiently large absorption the dependence of the output power on the natural frequency of the resonator assumes the form shown in Fig. 3. Individual pulses are not resolved in Fig. 3, so that the light part of the oscillogram gives the envelope of the pulses. It is typical that the envelope of the pulse amplitudes describes a power peak at the center of the absorption line. This question is discussed in greater detail in^[5].

Further increase of the CO_2 pressure (and consequently of the absorption) leads to two different effects, depending on the cell-wall temperature. At relatively high temperature ($\sim 800^\circ\text{K}$), an increase of the absorption to 3–3.5% leads to the vanishing of the pulsations at the edges of the line (see Fig. 4). At lower temperatures, pulsations are observed over the entire emission line all the way to the vanishing of the generation.

The described changes of the output power could be repeated at any excitation level in the discharge tube, and to obtain the same regime it was necessary to have

FIG. 3. Envelope of output-power pulse amplitudes.

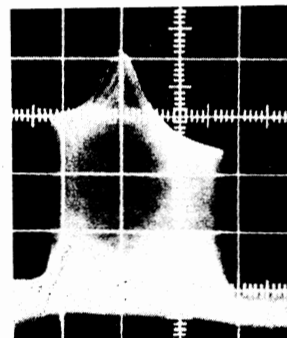
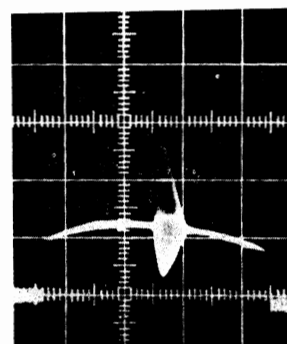


FIG. 4. Pulsation at the line center.



a larger absorption at a larger excess of gain over threshold. When working, for example, in the regime shown in Fig. 3, it was possible to go over to the regime shown in Fig. 2 by increasing the gain in the laser tube. On the other hand, by increasing the absorption in the absorbing cell it was possible to obtain the regime shown in Fig. 3. The pulse amplitude then increased with increasing gain.

The amplitude of each individual pulse exceeds by approximately one order of magnitude the level of the continuous power. The repetition frequency of the pulsations depends very strongly on the excess of gain over threshold, and for the case shown in Fig. 3 it could range from several dozen Hz to 50–60 kHz. The duration of the pulsations is practically independent of the excess of gain over threshold, and amounts to $\sim 10 \mu\text{sec}$. In those regimes where the pulsations were observed against the background of continuous generation (see, for example, Fig. 4), damped output-power oscillations of small amplitude appeared after each individual radiation pulse.

We now stop to discuss the measurements of the limit of onset of radiation pulsations as a function of the unsaturated absorption and of the gain. The limit of the instability was assumed to be the onset of regular pulsations at the line center. The dependence of the unsaturated gain in the amplifying tube on the discharge current was measured in a separate cell filled with a $\text{CO}_2\text{-N}_2\text{-He}$ mixture at a pressure equal to the pressure in the laser tube. The diameters of the laser tube and of the cell in which the gain was measured were equal within 0.1–0.2 mm. The maximum gain for 0.5 m was 25–28% at a discharge current 14 mA. The absorption was also measured in a separate quartz cell, the wall temperature of which was monitored with a calibrated thermocouple. Since the absorption coefficient of CO_2 at 800°K is small and amounts to $\sim 0.0014 \text{ cm}^{-1} \text{ Torr}^{-1}$, the measurements were performed

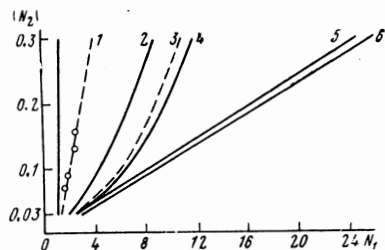


FIG. 5. Experimental (curve 1) and theoretical limits of the stability region. The theoretical curves correspond to the following values of the parameters of the amplifying and absorbing medium and of the resonator:

| | $\tilde{\Gamma}_1$ | $\tilde{\Gamma}_2$ | $\delta\omega$, MHz |
|---|--------------------|--------------------|----------------------|
| 2 | $2 \cdot 10^{-3}$ | $2 \cdot 10^{-2}$ | 50 |
| 3 | 10^{-3} | 10^{-2} | 5 |
| 4 | 10^{-3} | 10^{-2} | 50 |
| 5 | 10^{-3} | 10^{-1} | 5 |
| 6 | 10^{-3} | 10^{-1} | 50 |

at pressures higher than the ones we used in the laser absorbing cell (2–3 Torr). In this pressure range, the absorption coefficient still depends linearly on the CO₂ pressure^[13]. Knowing the dependence of the absorption on the CO₂ pressure in the absorption cell, it is easy to find the limit of onset of pulsations. Figure 5 (curve 1) shows the experimentally plotted boundary of the instability region. The ordinates represent the unsaturated gain and the absorption, referred to the losses in the resonator. The losses in the resonator were determined by measuring the threshold current, and a value $\sim 10\%$ was obtained. It is seen from Fig. 5 that introduction of absorption amounting to 0.1 of the excess of gain over threshold into the laser resonator leads to occurrence of regular pulsations.

3. THEORETICAL ANALYSIS

Let us consider a molecular system having vibrational (indices m, n) and rotational (J) states. In accordance with the typical conditions, we shall assume that the field interacts only with one rotational-vibrational transition $m, J_0 \rightarrow n, J_0 + 1$. As is well known, the most probable processes in molecule collisions are the changes of the velocity $\mathbf{v}' \rightarrow \mathbf{v}$ and of the rotational state $J' \rightarrow J$. These will be the processes taken into account below. Vibrational relaxation is apparently much less probable, and is disregarded. The collision frequency, generally speaking, depends on \mathbf{v} and J , and the kernels of the collision integrals, which determine the probability of the process, $A_j(J', \mathbf{v}', J, \mathbf{v})$, depend on both the initial and the final states. We shall consider, however, the simplest “strong-collision” model^[14], when each collision leads to an equilibrium distribution of the populations with respect to \mathbf{v} and with respect to J , i.e.,

$$A_j(\mathbf{v}', J', \mathbf{v}, J) = \tilde{\nu}_j W_M(\mathbf{v}) W_B(J), \quad (1)$$

where $\tilde{\nu}_j$ is the “arrival” frequency, which does not depend on \mathbf{v} or J ; W_M and W_B are the Maxwell and Boltzmann distribution functions. Thus, the initial system of equations for the elements $\rho_{jJ, j'J'}$ of the density matrix, describing the interaction between the molecules and the field, is

$$\left[\frac{\partial}{\partial t} + \mathbf{v}\nabla + \Gamma_m \right] \rho_{mJ, mJ} = \tilde{\nu}_m W_M(\mathbf{v}) W_B(J) \sum_{J'} \int d\mathbf{v}' \rho_{mJ', mJ'}(\mathbf{v}') \quad (2)$$

$$\begin{aligned} & + 2 \operatorname{Re} [i \rho_{mJ, nJ+1} V^*] + q_m(\mathbf{v}, J), \\ \left[\frac{\partial}{\partial t} + \mathbf{v}\nabla + \Gamma_n \right] \rho_{nJ+1, nJ+1} & = \tilde{\nu}_n W_M(\mathbf{v}) W_B(J) \sum_{J'} \int d\mathbf{v}' \rho_{nJ'+1, nJ'+1}(\mathbf{v}') \\ & - 2 \operatorname{Re} [i \rho_{mJ, nJ+1} V^*] + q_n(\mathbf{v}, J+1), \\ \left[\frac{\partial}{\partial t} + \mathbf{v}\nabla + \Gamma \right] \rho_{mJ, nJ+1} & = iV [\rho_{mJ, mJ} - \rho_{nJ+1, nJ+1}], \end{aligned}$$

where

$$\begin{aligned} V &= -\frac{d}{2\hbar} \mathcal{E} e^{-i\Omega t} \cos kx, \quad \Omega = \omega - \omega_0, \\ \Gamma_j &= \Gamma_j' + \nu_j, \quad \Gamma = \Gamma' + \nu; \end{aligned}$$

ω and ω_0 are the frequencies of the field and of the transition, d is the matrix element of the dipole moment, and \mathcal{E} is the field amplitude. The quantities Γ_n' , Γ_m' , and Γ' are the decay rates not connected with the collisions (i.e., spontaneous decay and diffusion to the walls), ν_j is the collision frequency of “departure” from the state \mathbf{v}, J ; $q_j(\mathbf{v}, J)$ is the relative number of excitation acts per unit volume.

This model can actually be used also in those cases when the width of the kernel $A_j(\mathbf{v}', J', \mathbf{v}, J)$ is several times smaller than the widths of the equilibrium distributions W_M and W_B . To this end it is necessary, however, that a large number of collisions, as a result of which the distribution “has time” to enter in equilibrium, occur within the characteristic time τ_n of the variation of the field amplitude $\mathcal{E}(t)$. In the experiment described above, this last condition is satisfied, since $\tilde{\nu}_j \sim 10^7 - 10^8$, $\tau_n \approx 10^{-5}$ sec, and the number of collisions of interest to us is $\tilde{\nu}_j \tau_n \sim 10^2 - 10^3$.

The system of equations (2) is very complicated. To simplify it we shall use two circumstances. First, we neglect the spatial inhomogeneity of the medium due to saturation^[15], i.e., we put

$$V \rho_{jj} = 0, \quad \rho_{mJ, nJ+1} = \rho^+ e^{ikx} + \rho^- e^{-ikx}. \quad (3)$$

Within the framework of the model (2), the right-hand sides of the equations for the populations contain the integral populations of the vibrational states

$$N_j = \sum_{J'} \int d\mathbf{v}' \rho_{jJ', jJ'}(\mathbf{v}'). \quad (4)$$

Using the condition (3), we supplement the system (2) with an equation for N_j :

$$\left[\frac{\partial}{\partial t} + \tilde{\Gamma}_j \right] N_j = \pm \operatorname{Re} [iG^* \langle \rho \rangle] + Q_j; \quad (5)$$

$\rho = \rho^+ + \rho^-$, $q_j = Q_j W_M(\mathbf{v})$, $\tilde{\Gamma}_j = \Gamma_j' + \nu_j - \tilde{\nu}_j$, $G = d\mathcal{E}/2\hbar$. $\tilde{\Gamma}_j$ is obviously the rate of decay of the vibrational state $j = m, n$. Under typical conditions, $\tilde{\Gamma}_j \sim 10^3 - 10^5$ sec⁻¹^[16], i.e., it is much smaller than ν_j or $\tilde{\nu}_j$.

The second simplifying assumption is that the damping constants of the vibrational states be equal:

$$\tilde{\Gamma}_m = \tilde{\Gamma}_n = \tilde{\Gamma}. \quad (6)$$

It will become clear subsequently that assumptions (3) and (6) do not change the qualitative aspect of the phenomena, although they can exert an influence on the quantitative results.

We use, finally, the fact that $\Gamma, \Gamma_j \gg \tilde{\Gamma}_j, 1/\tau_n$. This condition means that ρ_{ij} can “follow” the variation of

the field in a quasistatic manner, and the total populations N_j cannot. Mathematically this means that the derivatives with respect to t can be discarded everywhere except in the equations for N_j .

After a number of algebraic transformations and after introducing the new variables

$$\begin{aligned} z &= \frac{|G|^2 \tau}{\Gamma' + \nu}, & B &= \frac{4\pi\omega_{mn}}{h} |d|^2, & \tau &= \frac{1}{\Gamma_m} + \frac{1}{\Gamma_n} \\ N &= \frac{B(n_m^0 - n_n^0)}{\delta\omega} I(0), & n_j^0 &= \frac{Q_j}{\Gamma_j}, \\ x_j &= \frac{BI(0)}{\delta\omega} (N_j - n_j^0), & x &= x_m - x_n, & \gamma &= \frac{\bar{\nu}_m}{\Gamma_m} + \frac{\bar{\nu}_n}{\Gamma_n}, \end{aligned}$$

$$\begin{aligned} J(x) &= \frac{I(x)}{I(0)}, & I(x) &= \frac{1}{2} \int_{-\infty}^{\infty} \left[\frac{\Gamma}{\Gamma^2 + (\Omega - kv)^2} + \frac{\Gamma}{\Gamma^2 + (\Omega + kv)^2} \right] \\ &\times \left[1 + \frac{z}{2} \left(\frac{\Gamma^2}{\Gamma^2 + (\Omega - kv)^2} + \frac{\Gamma^2}{\Gamma^2 + (\Omega + kv)^2} \right) \right]^{-1} W_B(v) dv, * \end{aligned}$$

we obtain the simplified equation

$$\dot{x} + \tilde{\Gamma}x = -W_B(J) \frac{\Gamma}{\tau} I(0) J(x) z (N + \gamma x). \quad (7)$$

The physical meaning of x , N , $\delta\omega$, and κ consists in the following: N is the unsaturated population difference of the vibrational levels interacting with the field; x is the change in the difference of the populations of the same levels as a result of interaction with the field and rotational relaxation; the parameter κ is proportional to the field intensity and characterizes the "inhomogeneous" saturation; $\delta\omega$ is the rate of damping of the field in the resonator.

Supplementing Eq. (7) by the abbreviated equation for the field energy, we write down a system of equations for a laser with an absorbing cell (the indices 1 and 2 pertain to the amplifying and absorbing cells, respectively):

$$\begin{aligned} \dot{z} + z\delta\omega &= z\delta\omega W_B(J) \{J_1(z) [N_1 + \gamma_1 x_1] + J_2(\beta z) [N_2 + \gamma_2 x_2]\}, \\ \dot{x}_1 + \tilde{\Gamma}_1 x_1 [1 + c_1 z J_1(z)] &= -W_1 \frac{\Gamma_1}{\tau_1} I_1(0) z J_1(z) N_1, \\ \dot{x}_2 + \tilde{\Gamma}_2 x_2 [1 + c_2 z J_2(\beta z)] &= -W_2 \frac{\Gamma_2}{\tau_2} I_2(0) \beta z J_2(\beta z) N_2, \end{aligned} \quad (8)$$

here

$$c_1 = W_1 \Gamma_1 I_1(0) \gamma_1 / \tilde{\Gamma}_1 \tau_1, \quad c_2 = W_2 \Gamma_2 I_2(0) \gamma_2 \beta / \tilde{\Gamma}_2 \tau_2. \quad (9)$$

In the equation for κ , the expression in the curly brackets characterizes the saturated gain. In this model there are two different saturation mechanisms. The factors $J_1(\kappa)$ and $J_2(\beta\kappa)$ determine the saturation without allowance for relaxation with respect to ν and J , i.e., the so-called "inhomogeneous saturation," which in our approximation "follows" the field intensity in a quasistationary manner. On the other hand, the terms $\gamma_1 x_1$ and $\gamma_2 x_2$ determine the decrease of the population as a result of rotational relaxation and relaxation with respect to ν . The terms $c_1 \kappa J_1(\kappa)$ obviously determine the acceleration of the relaxation due to the field equalization of the population. The structure of the coefficients c_i is quite understandable. A decrease of the level populations $J' \neq J$ occurs only because after the collision the molecule turns out to be at the level J with a probability proportional to W_B . Therefore $c_i \propto W_B$. The product $\Gamma_i I_i(0)$ in c_i has the same physical meaning, but with respect to the velocity ν . When $\Gamma \ll \mathbf{k} \cdot \nu$ we

have $\Gamma_i I_i(0) = \sqrt{\pi} \Gamma_i / \mathbf{k}\nu$, i.e., $\Gamma_i I_i(0)$ is the probability that the molecule velocity after the collision will lie in the interval of the resonant velocities effectively interacting with the field. The combination $\gamma_i / \Gamma_i \tau_i$ characterizes the mean number of collisions during the lifetime $\tilde{\Gamma}_i^{-1}$ of the molecules. Finally, the factors $J_i(\kappa)$ reflect the fact that the equalization of the populations as a result of collisions also decreases with increasing "inhomogeneous" saturation. The right-hand sides in the equations for x_1 and x_2 have similar structures that are made clear by the statements made above.

It is appropriate to compare our model and the pure two-level model used in^[12]. The system of equations considered in^[12] has the following form (in our notation):

$$\begin{aligned} \dot{z} + \delta\omega z &= \delta\omega z [N_1 + x_1 + N_2 + x_2], \\ \dot{x}_1 + \tilde{\Gamma}_1 x_1 &= -\kappa \tilde{\Gamma}_1 [N_1 + x_1], \\ \dot{x}_2 + \tilde{\Gamma}_2 x_2 &= -\kappa \beta \tilde{\Gamma}_2 [N_2 + x_2]. \end{aligned} \quad (10)$$

The most significant difference between (10) and (8) lies in the absence of the factors $J_i(\kappa)$ ("inhomogeneous" saturation). It will be made clear by the subsequent analysis that for many conditions of practical interest the difference of $J_i(\kappa)$ from unity plays a decisive role. A second feature of (10) concerns the coefficients in the equations for x_i . Putting $\gamma_i = 1$ and redefining the quantity κ and the parameter β , we can obviously reduce (8) to (10) (provided $J_i(\kappa) = 1$):

$$\gamma_i = 1, \quad \kappa \leftarrow [W_i \Gamma_i I_i(0) / \tilde{\Gamma}_i \tau_i] \kappa, \quad \beta \leftarrow \frac{W_1 \Gamma_2 \tau_1 I_1(0)}{W_2 \Gamma_1 \tau_2 I_2(0)} \beta.$$

Such a substitution, just like the condition $J_i(\kappa) = 1$, denotes such a rapid relaxation with respect to ν and J that each rotational line and the entire rotational-vibrational band are "homogeneously" saturated.

We proceed to an analysis of the system (8). Putting in the equations $\dot{\kappa} = \dot{x}_1 = \dot{x}_2 = 0$, we obtain the stationary values of the quantities κ , x_1 , and x_2 . It is seen from (8) that there exist two types of equilibrium positions. The first, $\kappa = 0$, corresponds to the absence of generation, while the second, defined by the condition

$$\frac{N_1}{J_1^{-1} + c_1 \kappa} + \frac{N_2}{J_2^{-1} + c_2 \kappa} = 1, \quad (11)$$

corresponds to a monochromatic generation regime. It is seen from (11) that generation is possible when $N_1 + N_2 > 1$ (the N_i are expressed in threshold units). If cell 2 is absorbing, then $N_2 < 0$ and $N_1 > 1 + |N_2|$, i.e., the presence of $|N_2|$ denotes an increase of the threshold value of N_1 owing to the absorption in cell 2. If we put $J_1(\kappa) = J_2(\beta\kappa) = 1$ in (11), then we obtain the usual generation condition for the case of homogeneously broadened lines, but the saturation coefficients are determined by the relaxation time, by the Doppler width, and by the Boltzmann factor $W_B(J)$ (see the discussion of (8) and (10)). In the general case, the stationary value of κ is determined both by the "inhomogeneous" ($J_i \neq 1$) and by the "homogeneous" ($c_i \neq 0$) saturation. The qualitative course of the solution $\kappa(N_1, N_2)$ of Eq. (11) is shown in Fig. 6 for several values of $|N_2|$.

Linearizing the system (8) near the equilibrium position (11) and specifying it by means of a solution in the form $e^{\alpha t}$, we obtain the characteristic equation for the exponent α :

$$\alpha^3 + a_1 \alpha^2 + a_2 \alpha + a_3 = 0,$$

* $\mathbf{k}\nu = \mathbf{k} \cdot \mathbf{V}$.

$$a_1 = \tilde{\Gamma}_1[1 + c_1 \kappa J_1(\kappa)] + \tilde{\Gamma}_2[1 + c_2 \kappa J_2(\beta \kappa)] + \delta \omega \left[1 - \frac{N_1(\kappa J_1)'}{1 + c_1 \kappa J_1} + \frac{|N_2|(\kappa J_2)'}{1 + c_2 \kappa J_2} \right], \quad (12)$$

$$a_2 = \{ \tilde{\Gamma}_1[1 + c_1 \kappa J_1(\kappa)] + \tilde{\Gamma}_2[1 + c_2 \kappa J_2(\beta \kappa)] \} \delta \omega \left[1 - \frac{N_1(\kappa J_1)'}{1 + c_1 \kappa J_1} + \frac{|N_2|(\kappa J_2)'}{1 + c_2 \kappa J_2} \right] + \tilde{\Gamma}_1 \tilde{\Gamma}_2 [1 + c_1 \kappa J_1(\kappa)] \left[1 + c_2 \kappa J_2(\beta \kappa) + \delta \omega \kappa \tilde{\Gamma}_1 c_1 J_1(\kappa) \frac{N_1(\kappa J_1)'}{1 + c_1 \kappa J_1(\kappa)} - \delta \omega \kappa \tilde{\Gamma}_2 c_2 J_2(\beta \kappa) \frac{|N_2|(\kappa J_2)'}{1 + c_2 \kappa J_2(\beta \kappa)} \right], \quad (13)$$

$$a_3 = \tilde{\Gamma}_1 \tilde{\Gamma}_2 \delta \omega \kappa [1 + c_1 \kappa J_1(\kappa)] [1 + c_2 \kappa J_2(\beta \kappa)] \times \frac{d}{d\kappa} \left[1 - \frac{N_1 J_1}{1 + c_1 \kappa J_1} + \frac{|N_2| J_2}{1 + c_2 \kappa J_2} \right]. \quad (14)$$

For the investigated stationary generation regime to be stable, it is necessary that all the coefficients of the equation for α satisfy the Hurwitz-Routh conditions, namely

$$D_1 = a_1 > 0, \quad D_2 = a_1 a_2 - a_3 > 0, \quad D_3 = D_2 a_3 > 0. \quad (15)$$

We start the analysis of the inequalities (15) from the condition $D_3 = D_2 a_3 > 0$. Let us assume that $D_2 > 0$, and then we obtain an instability with respect to D_3 when $a_3 < 0$. From expression (14) for a_3 we see that $a_3 < 0$ denotes an increase of the effective gain of the system with increasing field intensity. In other words, the inequality $a_3 < 0$ determines the instability of the so-called "hysteresis" type, which was considered in^[9-11].

Near the generation threshold, the condition $a_3 < 0$ takes the form

$$|N_2| > \left(\frac{c_2 + |J_2'|}{c_1 + |J_1'|} - 1 \right)^{-1}. \quad (16)$$

The region $d\kappa/dN_1 < 0$ is the hysteresis region. If $\Omega = 0$ and $\Gamma_1 \ll \kappa \bar{v}_1$, then $J_1 = (1 + \kappa)^{-1/2}$, $J_2 = (1 + \beta \kappa)^{-1/2}$, and the inequality (16) goes over into

$$|N_2| > \left[\frac{c_2 + \beta/2}{c_1 + 1/2} - 1 \right]^{-1}, \quad (17)$$

which coincides when $c_1 = c_2 = 0$ with the hysteresis condition obtained in^[11]. If $c_2 \gg \beta/2$ and $c_1 \gg 1/2$, then the hysteresis is due to the purely "homogeneous" saturation. The numerical calculations for the parameters of the laser used in the experiments described above (Sec. 2) did not result in an instability of the hysteresis type; nor were phenomena characteristic of hysteresis observed in experiment.

We proceed to analyze the first instability condition $D_1 = a_1 < 0$, the physical meaning of which is as follows. According to (12), a_1 is the sum of the damping constants in the linearized equations for the populations (first and second terms) and the field (third term). The instability with respect to a_1 is determined by the fact that one of the functions κ , x_1 , or x_2 has "negative damping." This pertains obviously to the field intensity, since the damp-

ing constants in the linearized equations for the populations are always positive. It is easily seen from (12) that when $J_1 = J_2 = 1$ we have $a_1 > 0$, i.e., the instability with respect to a_1 can arise only when account is taken of the "inhomogeneous" saturation. Near the generation threshold there follows from (12) the following limitation for $|N_2|$:

$$\frac{c_2 + |J_2'|}{c_1 + |J_1'|} - 1 > |N_2| > \left(1 + \frac{\tilde{\Gamma}_1}{\delta \omega} c_1 + \frac{\tilde{\Gamma}_2}{\delta \omega} c_2 \right) / \left(\frac{|J_2'|}{|J_1'|} - 1 \right). \quad (18)$$

For the conditions of the experiments of Sec. 2 we have $\tilde{\Gamma}_1 c_1 \ll \delta \omega$, and the right-hand inequality in (18) coincides with the hysteresis condition (16) at $c_1 = c_2 = 0$ (purely "inhomogeneous" saturation). Thus, if we neglect the stabilizing influence of the population damping (the terms $\tilde{\Gamma}_1 c_1 / \delta \omega$), then the instability with respect to a_1 corresponds to hysteresis at the "inhomogeneous" saturation. Physically this is quite understandable. In our model, the saturation due to the rotational relaxation is the process with the highest inertia. Therefore during the initial period of the existence of the small deviations from the stationary regime, the system behaves as if there were no rotational relaxation, and strives to fall on the second branch of the hysteresis curve, which was calculated for the "inhomogeneous" saturation. With increasing κ , however, rotational relaxation comes into play, increasing the saturation and returning the system to smaller values of κ .

It is appropriate to emphasize that there is no instability of this type within the framework of the model (10).

The condition $D_2 = a_1 a_2 - a_3 < 0$ is more stringent than $a_1 < 0$, since in the vicinity of $a_1 = 0$, where we already have $a_1 > 0$, we get $D_2 < 0$ when $a_3 > 0$ (absence of hysteresis), i.e., there is no instability with respect to a_1 , but there exists instability with respect to D_2 .

Let us examine D_2 in the region of small κ . Expanding the expression for D_2 in powers of κ and retaining only the linear terms, we obtain

$$D_2 = \tilde{\Gamma}_1 \tilde{\Gamma}_2 (\tilde{\Gamma}_1 + \tilde{\Gamma}_2) - \tilde{\Gamma}_1 \tilde{\Gamma}_2 \delta \omega \kappa \left\{ |N_2| \left[\frac{(\tilde{\Gamma}_1 + \tilde{\Gamma}_2)^2}{\tilde{\Gamma}_1 \tilde{\Gamma}_2} (|J_2'| - |J_1'|) + \frac{\tilde{\Gamma}_2}{\tilde{\Gamma}_1} c_2 - \frac{\tilde{\Gamma}_1}{\tilde{\Gamma}_2} c_1 \right] - \frac{(\tilde{\Gamma}_1 + \tilde{\Gamma}_2)^2}{\tilde{\Gamma}_1 \tilde{\Gamma}_2} |J_1'| - \frac{\tilde{\Gamma}_1}{\tilde{\Gamma}_2} c_1 \right\}. \quad (19)$$

Thus, if $|N_2|$ is sufficiently large

$$|N_2| > \left[\frac{|J_2'| + \tilde{\Gamma}_2^2 c_2 / (\tilde{\Gamma}_1 + \tilde{\Gamma}_2)^2}{|J_1'| + \tilde{\Gamma}_1^2 c_1 / (\tilde{\Gamma}_1 + \tilde{\Gamma}_2)^2} - 1 \right]^{-1} = |N_2|_{\text{cr}}, \quad (20)$$

then D_2 may turn out to be negative and the stationary regime may turn out to be unstable. From (19) and (11) we easily find that the break in the stationary generation will occur at

$$N_1 - (1 + |N_2|) > \frac{|N_2|}{|N_2|_{\text{cr}} - 1} \frac{\tilde{\Gamma}_1 \tilde{\Gamma}_2}{\delta \omega (\tilde{\Gamma}_1 + \tilde{\Gamma}_2)} \frac{|J_1'| + c_1}{|J_1'| + c_1 \tilde{\Gamma}_1^2 / (\tilde{\Gamma}_1 + \tilde{\Gamma}_2)^2}. \quad (21)$$

Since $\tilde{\Gamma}_1 / \delta \omega$, $\tilde{\Gamma}_2 / \delta \omega \sim 10^{-4} - 10^{-5}$, condition (21) corresponds to an exceedingly small excess of gain over the threshold value even at $|N_2| / |N_2|_{\text{cr}} - 1 \sim 0.01$. It is therefore perfectly natural that the pulsation regime occurs directly at the threshold as soon as $|N_2|$ exceeds the critical value $|N_2|_{\text{cr}}$. The numerical value of $|N_2|_{\text{cr}}$ calculated from formula (20) for the conditions of the experiment described above turned out to be 0.2%.

From a comparison of (20) and (16) it is easily seen

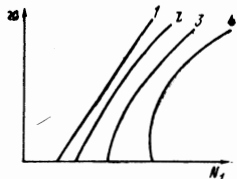


FIG. 6. Qualitative course of the solution $\kappa(N_1, N_2)$ of Eq. (11): curve 1— $N_2 = 0$, curves 2, 3, and 4 correspond to an increase of $|N_2|$.

that $|N_2|_{CR}$ is larger than that value of $|N_2|$ which is necessary for hysteresis due to inhomogeneous saturation ($c_1 = c_2 = 0$ in (16)). This makes the interpretation given above for the instability in question quite lucid, namely, the intensity pulsations constitute a transition of the system between the $\kappa(N_1, N_2)$ curve constructed in the absence of rotational relaxation, $c_1 = c_2 = 0$, and the same curve at $c_1 \neq 0$ and $c_2 \neq 0$. Since $J_1, J_2 \sim 1$ and $c_1, c_2 \gg 1$, the power at the peak of the pulse is much larger than the power of the stationary generation, which likewise agrees with experiment. In the region $(|J_2|/|J_1| - 1)^{-1} < N_2 < |N_2|_{CR}$, hysteresis due to "inhomogeneous" saturation is already possible, but the stationary generation regime is still stable. In this region of $|N_2|$, according to our interpretation of the phenomena, the process of establishment of the stationary regime can obviously have the form of damped oscillations. This corresponds fully to the transient pulsations observed in the region of 0.7–2.5% absorption (Sec. 2).

Thus, the considered laser model (with allowance for rotational relaxation and relaxation with respect to the velocities v) contains regimes of damped and regular pulsations, i.e., it explains the experimental data qualitatively. Besides the very existence of two pulsation regimes, the model also accounts correctly for their sequence with increasing absorption. It must be stated, however, that the quantitative results agree only in order of magnitude. For example, according to the calculation, the damped and regular oscillations should be observed at absorptions exceeding 0.02 and 0.2%, respectively. The experimental values, however, were 0.7 and 2%. Apparently this discrepancy is due to our simplifications of the model (equality of the lifetimes of the upper and lower vibrational states, the strong-collision model), but does not negate the role of rotational relaxation.

At large κ , an analysis of the Hurwitz-Routh conditions is difficult, because of the complexity of these conditions. Therefore the upper limit of the unstable regime was calculated numerically with a computer. It turned out, in accord with the experiment, that at fixed $|N_2| > |N_2|_{CR}$ the stationary generation is unstable only at sufficiently small excesses of the saturated gain over threshold. The upper limit (with respect to N_1) of the stability region was calculated. Curves 2–5 in Fig. 5

represent the results of the calculation for different values of the laser parameters $\delta\omega$, $\tilde{\Gamma}_2$, and $\tilde{\Gamma}_1$. It is seen from Fig. 5 that the upper limit of the region of instability with respect to N_2 changes little with changing $\delta\omega$ and is very sensitive to changes of $\tilde{\Gamma}_1$ and $\tilde{\Gamma}_2$. Curve 1 on Fig. 5 is experimental. Taking into account the relatively crude character of the model, the agreement with experiment can be regarded as satisfactory.

¹A. A. Mak, R. A. Anan'ev and B. A. Ermakov, Usp. Fiz. Nauk **92**, 373 (1967) [Sov. Phys.-Uspekhi **10**, 419 (1968)].

²O. R. Wood and S. E. Schwars, Appl. Phys. Lett. **11**, 88, 1968.

³N. V. Karlov, T. P. Kuz'min, Yu. I. Petrov and A. M. Prokhorov, ZhETF Pis. Red. **7**, 174 (1968) [JETP Lett. **7**, 134 (1968)].

⁴P. L. Hanst, J. A. Morreal and W. J. Nenson, Appl. Phys. Lett. **12**, 58, 1968.

⁵Yu. V. Brzhazovskii, L. S. Vasilenko and V. P. Chebotaev, Zh. Eksp. Teor. Fiz. **55**, 2095 (1968) [Sov. Phys.-JETP **28**, 1108 (1969)].

⁶T. J. Chang and C. N. Wong, Appl. Phys. Lett. **15**, 157, 1969.

⁷S. Marcus, Appl. Phys. Lett. **15**, 361, 1969.

⁸J. Ohtsuka and H. Joshinaga, Japan J. Appl. Phys. **8**, 1319, 1969.

⁹V. I. Lisitsyn and V. P. Chebotaev, Zh. Eksp. Teor. Fiz. **54**, 419 (1968) [Sov. Phys.-JETP **27**, 227 (1968)].

¹⁰V. N. Lisitsyn and V. P. Chebotaev, ZhETF Pis. Red. **7**, 3 (1968) [JETP Lett. **7**, 1 (1968)].

¹¹A. P. Kazantsev, S. G. Rautian and G. I. Surdutovich, Zh. Eksp. Teor. Fiz. **54**, 1409 (1968) [Sov. Phys.-JETP **27**, 759 (1968)].

¹²V. I. Bepalov and E. I. Yakubovich, Izv. Vuzov, Radiofizika **8**, 5 (1965).

¹³T. Gerry and D. A. Leonard, Appl. Phys. Lett. **8**, 227, 1966.

¹⁴S. G. Rautian and I. I. Sobel'man, Usp. Fiz. Nauk **90**, 209 (1966) [Sov. Phys.-Uspekhi **9**, 701 (1967)].

¹⁵S. G. Rautian, Trudy FIAN **43** (1968), p. 3.

¹⁶P. K. Cheo, J. Appl. Phys. **38**, 3563, 1967.

Translated by J. G. Adashko